ONLINE FIRST

This is a provisional PDF only. Copyedited and fully formatted versión will be made available at final publication

HISTOLOGY AND HISTOPATHOLOGY

ISSN: 0213-3911
e-ISSN: 1699-5848

Differential roles of serotonin receptor subtypes in regulation of neurotrophin receptor expression and intestinal hypernociception

Authors: Meng-Ping She, Yu-Ting Hsieh, Li-Yu Lin, Chia-Hung Tu, Ming-Shiang Wu, Ling-Wei Hsin and Linda Chia-Hui Yu

DOI: 10.14670/HH-18-687
Article type: ORIGINAL ARTICLE
Accepted: 2023-12-11
Epub ahead of print: 2023-12-11

Differential roles of serotonin receptor subtypes in regulation of neurotrophin receptor expression and intestinal hypernociception

Meng-Ping She[1], Yu-Ting Hsieh[1], Li-Yu Lin[1], Chia-Hung Tu[2], Ming-Shiang Wu[2], Ling-Wei Hsin[3,4], and Linda Chia-Hui Yu[1]*

[1]Graduate Institute of Physiology, National Taiwan University College of Medicine; [2]Department of Internal Medicine, National Taiwan University Hospital and College of Medicine;
[3]School of Pharmacy, National Taiwan University;
[4]Center for Innovative Therapeutics Discovery, National Taiwan University, Taipei, Taiwan ROC.

***Corresponding author:**
Linda Chia-Hui Yu, Professor
Graduate Institute of Physiology, National Taiwan University College of Medicine
Suite 1020, #1 Jen-Ai Rd. Sec. 1, Taipei 100, Taiwan ROC
TEL: 886-2-23123456 ext: 288237
E-mail: lchyu@ntu.edu.tw

Running title: Gut hyperalgesia via 5-HT_7 activation

Conflict of Interest: The authors have no conflicts of interest to declare.

Abbreviations: IBS, Irritable bowel syndrome; 5-HT_7, 5-hydroxytryptamine receptor subtype 7; PGP9.5, protein gene product 9.5; NGF, nerve growth factor; BDNF, brain-derived nerve growth factor; Trk, Tropomyosin receptor kinase; $p75^{NTR}$, p75 neurotrophin receptor; TNBS, 2,4,6-trinitrobenzene sulfonic acid; PFA, paraformaldehyde; VMR, visceromotor response; CRD, colorectal distension; AUC, area under curve; LPM, loperamide; ALN, alosetron.

Declarations

- **Ethics approval:** All experimental procedures were approved by the Institute of Animal Care and Use Committee (20160288) of NTUCM.
- **Competing interests:** The authors declare that they have no competing interests.

- **Availability of data and material:** The data and material are available upon request.
- **Funding:** This study was supported by grants from the National Science and Technology Council (NSTC 111-2622-B-002-016), Ministry of Science and Technology (MOST 110-2622-B-002-013, MOST 110-2320-B-002-011-MY3), National Research Program for Biopharmaceuticals, National Science Council (NSC100-2325-B-002-035, 101-2325-B-002-031, 102-2325-B-002-030), National Health Research Institutes (NHRI-EX111/112/113-11108BI), and National Taiwan University SPARK projects, and Core consortium projects (NTUCC-109L893102, NTUCC-110L891202, NTUCC-111L890602, NTU-CC-112L895002).
- **Author contribution:** Guarantors of the integrity of the entire study: LCY; study concepts and design: LCY and LWH; data acquisition: MPS, YTH, LWL; data analysis/interpretation: MPS, YTH, LWL; statistical analysis: MPS, YTH, LWL; material and technical support: CHT, MSW; obtained funding: MSW, LWH, and LCY; manuscript drafting or revision for important intellectual content, literature research, manuscript editing, and manuscript final version approval: all authors.
- **Acknowledgments:** The authors thank the Animal Centre, Imaging Facility, and Biomedical Resource Core of the First Research Core Laboratory of NTUCM for technical assistance. *Giardia* trophozoites strain GS/M was a kind gift from the laboratory of Dr. Chin-Hung Sun at the Department of Tropical Medicine and Parasitology, National Taiwan University College of Medicine.

ABSTRACT

Objectives: Aberrant serotonin (5-hydroxytryptamine, 5-HT) metabolism and neurite outgrowth were associated with abdominal pain in irritable bowel syndrome (IBS). We previously demonstrated that 5-HT receptor subtype 7 (5-HT_7) was involved in visceral hypersensitivity of IBS-like mouse models. The aim was to compare the analgesic effects of a novel 5-HT_7 antagonist to reference standards in mouse models and investigate the mechanisms of 5-HT_7-dependent neuroplasticity.

Methods: Two mouse models, including *Giardia* post-infection combined with water avoidance stress (GW) and post-resolution of trinitrobenzene sulfonic acid-induced colitis (PT) were used. Mice were orally administered CYY1005 (CYY, a novel 5-HT_7 antagonist), alosetron (ALN, a 5-HT_3 antagonist), and loperamide (LPM, an opioid receptor agonist) prior to measurement of visceromotor responses (VMR). Levels of nerve growth factor (NGF), brain-derived neurotrophic factor (BDNF), and neurotrophin receptors (NTRs) were assessed.

Results: Peroral CYY was more potent than ALN or LPM in reducing VMR values in GW and PT mice. Increased mucosal 5-HT_7-expressing nerve fibers were associated with elevated *Gap43* levels in the mouse colon. We observed higher colonic *Ntrk2* and *Ngfr* expression in GW mice, and increased *Bdnf* expression in PT mice compared with control mice. Human SH-SY5Y cells stimulated with mouse colonic supernatant or exogenous serotonin exhibited longer nerve fibers, which CYY dose-dependently inhibited. Serotonin increased *Ntrk1* and *Ngfr* expression via 5-HT_7 but not 5-HT_3 or 5-HT_4, while *Ntrk2* upregulation was dependent on all three 5-HT receptor subtypes.

Conclusions: Stronger analgesic effects by peroral CYY were observed compared with reference standards in two IBS-like mouse models. The 5-HT_7-dependent NTR upregulation and neurite elongation may be involved in intestinal hypernociception.

Keywords: irritable bowel syndrome, nerve hypersensitivity, serotonin receptors, neurotrophin receptors, neurite outgrowth, enteric nervous system.

Introduction

Irritable bowel syndrome (IBS) is a functional bowel disorder in which relapsing abdominal pain or discomfort is associated with defecation or a change in bowel habit without detectable organic causes (Ford *et al.*, 2020; BouSaba *et al.*, 2022; Lambarth *et al.*, 2022). A lower pain threshold to intestinal distension, which is referred to as visceral hypersensitivity, was reported in all IBS patients, irrespective of the defecation patterns (Ford *et al.*, 2020; BouSaba *et al.*, 2022; Lambarth *et al.*, 2022). Altered intestinal serotonin/5-hydroxytryptamine (5-HT) metabolism, higher density of mucosal nerve fibers, and elevated levels of neurotrophins, such as nerve growth factor (NGF) and brain-derived neurotrophic factors (BDNF), are biomarkers correlative to abdominal pain scores in IBS patients (Atkinson *et al.*, 2006; Dunlop *et al.*, 2006; Yu *et al.*, 2012; Dothel *et al.*, 2015; Zhang *et al.*, 2019).

Serotonin is initially identified as a brain neurotransmitter, which is now recognized as mainly (95%) produced by enteric nerves and enterochromaffin cells involved in bowel movement and pain sensation with neuroendocrine functions. Elevated 5-HT-dependent visceral hypersensitivity was reported in recipient animals intracolonically infused with mucosal biopsy and fecal supernatant from IBS patients (Gao *et al.*, 2022), and administration of exogenous 5-HT caused intestinal hyperalgesia in rat models (Cenac *et al.*, 2010; Zhang *et al.*, 2011). Expression of 5-HT receptor subtype 3 (5-HT_3), subtype 4 (5-HT_4), and subtype 7 (5-HT_7) have been reported in the intestinal tract; 5-HT_7 is the most recently discovered member of the receptor family (Kim and Khan, 2014; Lee *et al.*, 2021). Our previous study demonstrated a reduction in intestinal pain by treatment with a novel 5-HT_7 antagonist, CYY1005 (CYY), in IBS-like mouse models (Chang *et al.*, 2022). Other clinical medications for diarrhea-predominant IBS included alosetron (ALN, a 5-HT_3 antagonist) and loperamide (LPM, an opioid receptor agonist), while tegaserod (a 5-HT_4 agonist) was used for the management of constipation-predominant IBS. ALN and tegaserod improve symptoms but have severe side effects such as cerebrovascular and cardiovascular ischemia (Ford *et al.*, 2009; Nee *et al.*, 2015). Opiate agonists such as LPM are commonly used to correct bowel movements by reducing the peristaltic rate (Corsetti and Whorwell, 2017). In light of the fact that current treatments are ineffective for pain symptoms in IBS, the analgesic effects of peroral CYY are compared to ALN and LPM in this study.

Increased transcript levels of 5-HT_3 and 5-HT_7 were documented in colorectal tissues of diarrhea-predominant IBS patients (Ren *et al.*, 2007; Zou *et al.*, 2007; Yu *et al.*, 2016), however, limited evidence of altered intestinal 5-HT_4 levels was found in IBS patients despite numerous studies using 5-HT_4 receptor agonists to target constipation symptoms (Fukudo *et al.*, 2021). The expression of 5-HT_7 was observed on enteric

neurons (Tonini *et al.*, 2005; Dickson *et al.*, 2010; Yaakob *et al.*, 2015), lumbar dorsal root ganglia, and brain cortex and hippocampus regions (Meuser *et al.*, 2002, Zou *et al.*, 2007). In contrast, 5-HT_3 and 5-HT_4 receptor expression was identified in enteric nerves (Liu *et al.*, 2005; Michel *et al.*, 2005; Monro *et al.*, 2005) and colonic epithelia (Ataee *et al.*, 2010; Spohn *et al.*, 2016). Recent reports demonstrated that 5-HT_3 was involved in serotonin-evoked ion secretion in mouse colonic organoids and epithelial 5-HT_4 activation increased fluid secretion in the proximal colon (Bhattarai *et al.*, 2017; Bhattarai *et al.*, 2018). These findings suggest that interventions targeting 5-HT_3 and 5-HT_4 may partly be acting on epithelial ion fluxes while targeting 5-HT_7 mainly corrects neural sensation.

Neuroplasticity is crucial for neuronal repair and synapse formation, and modulates the magnitude of pain sensation. Accumulating evidence indicates that nerve fiber outgrowth and neurotrophin levels are increased in the intestinal mucosa of IBS patients (Yu *et al.*, 2012; Dothel *et al.*, 2015; Zhang *et al.*, 2019). Neurotrophins such as NGF and BDNF bind to neurotrophin receptors (NTRs) composed of subunits including high-affinity receptors, i.e., tropomyosin receptor kinase (Trk) A and B, in complex with the low-affinity $p75^{NTR}$ (Khan and Smith, 2015). Previous work from our laboratory and others demonstrated that 5-HT_7 was involved in intestinal mucosal neurite outgrowth and forebrain synaptogenesis (Kobe *et al.*, 2012; Speranza *et al.*, 2017; Chang *et al.*, 2022). A role of 5-HT_4 was also documented in dendrite sprouting for memory formation (Schill *et al.*, 2020). To date, the differential roles of 5-HT receptor subtypes in regulating individual NTR subunit expression and neurite elongation remain unclear.

In the present study, two mouse models with visceral hypersensitivity were utilized to compare analgesic effects with peroral CYY against reference standards, such as ALN and LPM, clinically used for diarrhea-predominant IBS. Mucosal expression patterns of 5-HT receptor subtypes and the transcript levels of neurotrophins and NTRs were examined in mouse colonic tissues. The half-maximum inhibitory concentration (IC50) of CYY on neurite outgrowth was determined in human neuronal cell cultures stimulated with bacteria-free colonic supernatants *in vitro*, and was compared to that of a putative 5-HT_7 receptor antagonist (SB-269970) known to be unstable via oral routes. Moreover, the roles of 5-HT receptor subtypes in the regulation of distinct NTR subunits were assessed.

Materials and Methods

Animals

Specific pathogen-free C57BL/6 male mice (4-6 weeks of age) obtained from the National Taiwan University College of Medicine (NTUCM) animal facility were used for the study. Animals were raised in a temperature-controlled room (20 ± 2°C) with 12/12-hour light/dark cycles and fed with regular chow and water *ad libitum*. All experimental procedures have been approved by the Institute of Animal Care and Use Committee (IACUC#20160288) of NTUCM.

Reagents

A novel 5-HT_7 antagonist, CYY1005 (PCT# WO2018157233 (A1)), was chemically synthesized by the laboratory of Dr. Hsin LW, School of Pharmacy, NTU. Reagents, such as SB-269970 hydrochloride (SB7, a selective 5-HT_7 antagonist), ALN (a selective 5-HT_3 antagonist), and LPM (an agonist to mu-, delta-, and kappa-opioid receptors), were purchased from Sigma-Aldrich (St. Louis, MO, USA). GR125487 (a selective 5-HT_4 antagonist) was purchased from Tocris Bioscience (Minneapolis, MN, USA).

Mouse models of visceral hypersensitivity

Two mouse models of IBS-like visceral hypersensitivity were investigated, including one model with dual triggers of parasite postinfection combined with psychological stress, and the other one with post-resolution of 2,4,6-trinitrobenzene sulfonic acid (TNBS)-induced colitis (Feng *et al.*, 2012; Chen *et al.*, 2013; Lapointe *et al.*, 2015; Halliez *et al.*, 2016; Hsu *et al.*, 2016). In the first model, mice were inoculated with *Giardia* (G) trophozoites on day 0 and subjected to water avoidance stress (WAS) during the post-clearance phase on days 42-51 (designated the GW model) (Chen *et al.*, 2013; Hsu *et al.*, 2016). Briefly, mice were orogavaged with 10^7 *Giardia* trophozoites strain GS/M suspended in 0.2 ml of sterile saline. On the sixth week postinfection, when trophozoites cannot be detected in the intestine, mice were subjected to WAS for 1 hr/day for ten consecutive days, followed by measurement of intestinal pain on the last day of the stress session. The uninfected unstressed control (Ctrl) group was pair-fed with phosphate-buffered saline and left in cages unhandled.

In the second model, post-inflammatory pain was measured after the resolution of colitis induced by intracolonic injection of TNBS (Sigma) at 75 mg/kg body weight dissolved in 40% ethanol in a 0.2 ml volume of saline on day 0 (Feng *et al.*, 2012; Lapointe *et al.*, 2015; Halliez *et al.*, 2016). The sham control (sham) group was intracolonically injected with the same volume of saline on day 0. The time point of 24 days post-TNBS (designated the PT model) was chosen to represent persistent pain in

the absence of inflammation, whereby our pilot study demonstrated the resolution of inflammatory parameters (i.e., myeloperoxidase activity and histopathological scores) seven days after TNBS injection (Chang *et al.*, 2022). To test analgesic effects in the two models with visceral hypersensitivity, mice were perorally (p.o.) administered reagents at 5 mg/kg via a single dose in a saline vehicle 1.5 hours before intestinal pain measurement.

Assessment of pain sensation to colorectal distension

Abdominal pain was measured by visceromotor responses (VMRs) to colorectal distension (CRD) as previously described (Hong *et al.*, 2011; Hsu *et al.*, 2016; Chang *et al.*, 2022). Briefly, electrodes made from Teflon-coated stainless-steel wire (A-M Systems, Carlsborg, WA) were implanted in the abdominal external oblique muscles of mice at least 14 days before VMR experiments, and the electrodes were exteriorized onto the back of the neck. The surgical procedure was granted by IACUC#20160288. Mice were habituated in the plexiglass cylinder for 30 minutes per day for three consecutive days before VMR experiments for acclimatization. For recording, electrodes were connected to an electromyogram acquisition system (AD instruments, New South Wales, Australia). Mice were fasted overnight for the VMR tests, and the colon was distended by inflating a balloon catheter inserted intra-anally and subjected to four 10-second distensions (15, 40, and 65 mmHg) with 3-min rest intervals. The electromyographic (EMG) activity was amplified and digitized using a transducer (AD instruments) connected to a P511 AC amplifier (Grass Instruments, CA, USA) and Powerlab device with Chart 5 software (AD instruments). The EMG activity was rectified and the response was recorded as the increase in the area under the curve (AUC) of the EMG amplitude during CRD versus the baseline period.

Charcoal meal test

Mice were gavaged with 0.2 ml charcoal meal (3% arabic gum and 10% charcoal in PBS; Sigma) after the measurement of VMR. The intestinal tract was removed after thirty minutes and longitudinally dissected. Intestinal transit was defined as the position of the leading edge of the charcoal meal traveled as a percentage of the total length of the small and large intestine.

Histopathological examination

Intestinal tissues were fixed in 4% paraformaldehyde (PFA) and embedded in paraffin wax with proper orientation of the crypt to the villus axis before sectioning. Sections of 5-μm thickness were deparaffinized with xylene and graded ethanol, stained with hematoxylin and eosin, and observed under a light microscope (Pai *et al.*,

2021, 2023).

Immunofluorescent staining in intestinal tissues

Cryofixed sections post-fixed in acetone were incubated with 1% Triton X-100 for 10 minutes and then blocked with 1% bovine serum albumin (BSA) for two hours at room temperature. Tissue sections were incubated with primary antibodies, rabbit polyclonal anti-PGP9.5 (#39959) (1:250, GeneTex), anti-5-HT_7 (#ab61562) (1:200, Abcam, Burlingame, CA, USA), anti-5-HT_3 (#ab13897) (1:100, Abcam), anti-5-HT_4 (#ab60359) (1:200, Abcam), or isotype control IgG antibodies (#10500C, Invitrogen) overnight in a cold room (Matsumoto *et al.*, 2012; Dothel *et al.*, 2015). Negative controls by omitting primary antibodies were performed to confirm specific staining. The sections were washed with saline and incubated with a secondary goat anti-rabbit IgG conjugated to Alexa Fluor 488 (1:250, Invitrogen) for one hour at room temperature. Tissues were then incubated with a Hoechst dye (1 µg/ml in PBS) (Sigma) for 30 minutes. The images were captured under a Zeiss microscope for quantification of fluorescence intensity by using imaging software (Axio Vision SE64, Zeiss, Oberkochen, Germany). Fluorescence intensity per area was quantified in five images of the colonic mucosa per mouse and in five mice per group. A total of 25 images from each mouse group were used for comparison (Huang *et al.*, 2021; Pai *et al.*, 2021).

In addition, tissues were then double-stained with mouse monoclonal anti-PGP9.5 (1:800, Abcam) and rabbit polyclonal anti-5-HT_7 (1:200, Abcam), followed by secondary goat anti-rabbit or anti-mouse IgG conjugated to Alexa Fluor 488 or 546 (1:1000, Invitrogen) for one hour at room temperature. Tissues were then incubated with a Hoechst dye (1 µg/ml in PBS) (Sigma) for 30 minutes. The images were captured using a Zeiss microscope to verify the localization of PGP9.5 and 5-HT_7 immunostaining.

Western Blotting

Intestinal mucosal proteins were extracted with complete radio-immunoprecipitation assay buffer and subjected to electrophoresis (4-13% polyacrylamide). The resolved proteins were then electrotransferred onto polyvinylidene fluoride or nitrocellulose membranes in a semi-dry blotter. Blots were blocked with 5% (w/v) nonfat dry milk in Tris-buffered saline (TBS) or 5% (w/v) bovine serum albumin in TBS with Tween 20 (TBS-T; 0.1% (v/v) Tween-20 in TBS) for one hour, washed with TBS-T, and incubated with a primary antibody at 4°C overnight. The membrane was washed and incubated with a secondary antibody for one hour. After washing, the membranes were incubated with a chemiluminescent solution and signals were detected. The primary antibodies used included mouse monoclonal anti-

NGF (1:100, Santa Cruz) and rabbit polyclonal anti-BDNF (1:250, Santa Cruz). A mouse monoclonal anti-β-actin (1:5000, Sigma) was used as a loading control. The secondary antibodies used were horseradish peroxidase-conjugated goat, mouse, or rabbit anti-rabbit IgG (1:1000, Cell Signaling) (Kuo *et al.*, 2015; Kuo *et al.*, 2016).

Polymerase chain reaction (PCR)

Total RNA was extracted from whole colonic tissues and cell samples using Trizol reagent (Invitrogen) according to the manufacturer's instructions. The RNA (2 μg) was reverse transcribed with oligo$(dT)_{15}$ using RevertAid™ First Strand cDNA Synthesis kit (ThermoFisher, Waltham, MA, USA) in a 20 μL reaction volume. Quantitative PCR (qPCR) was performed using an Applied Biosystems StepOnePlus Real-Time PCR System (Applied Biosystems, Waltham, MA, USA). The reaction mixture consisted of 50 ng of RT product, 10 μL of Power SYBR Green PCR Master Mix, and 125 nM specific primer pairs in a final reaction volume of 20 μL. The qPCR primer pairs for mouse and human cells were designed in this study based on the National Center for Biotechnology Information (NCBI) nucleotide sequence of each gene. The protocol was programmed as follows: 95°C for 10 minutes for 1 cycle; 95°C for 15 seconds, and 60°C for 1 minute for 40 cycles. Each sample was run in duplicate, and the mean threshold cycle (Ct) was determined from the two runs. Gene expression was calculated from the difference of Ct between the target gene and endogenous housekeeping gene encoding for β-actin (*ACTB*) as ΔCt. Subsequently, the ΔΔCt values were calculated by subtracting the mean ΔCt of the control group from those of the experimental groups, and the relative gene expression is expressed as the fold difference ($2^{-\Delta\Delta Ct}$) (Huang *et al.*, 2019; Huang and Yu, 2020; Yu *et al.*, 2022).

In another setting, semi-quantitative PCR was performed to analyze growth-associated protein 43 (Gap43) expression in the colonic mucosal samples. The cDNA samples were added into a master mix containing 1X PCR buffer, 1 U DreamTaq™ DNA Polymerase, 0.2 mM dNTPs mixture, 0.4 μM forward primer, and 0.4 μM reverse primer. The DNA thermal cycler was programmed to perform a protocol as follows: 95°C for 3 min for 1 cycle; 95°C for 30 sec (denaturation), X°C for 30 sec (annealing, Tm), and 72°C for 30 sec (extension) for 30 cycles; and 72°C for 7 min for final extension. The PCR reaction was performed by using primer pairs for Gap43 (forward: 5'-AGCCAAGGAGGAGCCTAAAC-3' and reverse: 5'-TCAGGCATGTTCTTGGTCAG-3'; *Tm* = 54°C) and β-actin (forward: 5'-GGGAAATCGTGCGTGAC-3' and reverse: 5'-CAAGAAGGAAGGCTGGAA-3'; *Tm* = 55°C) (Dothel *et al.*, 2015). Negative controls were performed with samples that was not reverse transcribed. The PCR products were then electrophoresed in a 1.5% agarose gel in the presence of 0.5 μg/mL ethidium bromide, visualized with an ultraviolet transilluminator, and photographed. The intensity of the

DNA bands was analyzed using Gel-Pro Analyzer 4.0 software.

Cell cultures

Human neuroblastoma SH-SY5Y cells were used for the measurement of nerve fiber length and qPCR analysis as described (Dothel *et al.*, 2015; Hsu *et al.*, 2016; Chang *et al.*, 2022). For neurite length studies, cells were plated at 2 x 10^3 cells/ml overnight and treated with 10 μM all-trans retinoic acid (RA) (Sigma) daily for three days to induce differentiation. The cells were pretreated with CYY or SB7 at various concentrations ranging from 0.01 to 100 μM and then incubated with bacteria-free colonic supernatant (see below) in serum-free medium for four days by adding supernatant samples every two days for analysis of neurite outgrowth. The IC50 of compounds to suppress neurite outgrowth was calculated using GraphPad Prism software (GraphPad Software Inc., CA, USA).

In other settings, cells were stimulated with 1 μM serotonin (Sigma) in a reduced serum medium (2% FBS) for 48 hours for measurement of neurite length. For groups of combined treatment with neurotrophins, cells were stimulated with 1 μM serotonin in the presence of 100 ng/ml recombinant NGF (RD Systems) and recombinant BDNF (Sigma-Aldrich) in serum-free medium for 48 hours for measurement of neurite length. Alternatively, SH-SY5Y cells were seeded at a density of 1 x 10^5 cells/ml in 12-well plates overnight and were stimulated with 1 μM serotonin in the presence of antagonists to 5-HT receptor subtypes for quantitative PCR analysis.

Bacteria-free mouse colonic supernatant

Whole colonic tissues (1 cm) were homogenized in a serum-free medium at a ratio of 1 mg of tissue to 10 μl medium on ice as described (Hsu *et al.*, 2016; Chang *et al.*, 2022). One tablet of complete-Mini→ (C-M) (Roche, Mannheim, Germany) was dissolved in 10 ml of serum-free medium for tissue homogenization. The protease inhibitor cocktail was used to prevent the proteolytic activity of gut supernatant, which might cause cell death of SH-SY5Y cultures. Tissue lysate was centrifuged at 10000 · *g* for 10 min at 4°C and the supernatant was collected. The supernatant was mixed with 20-times volume of serum-free medium with C-M and passed through a sterilized filter with 0.45 μm pore size (Merck Millipore, Darmstadt, Germany). The bacteria-free supernatant was diluted with serum-free medium without C-M at a ratio of 1: 100 and then added to SH-SY5Y cells.

Analysis of neurite outgrowth

The measurement of nerve fiber length was performed following established protocols (Hsu *et al.*, 2016; Chang *et al.*, 2022). Briefly, SH-SY5Y cells were

photographed with a microscope equipped with a digital camera. The length of nerve fibers was determined using imaging software (ImageJ 1.47v). The average length of nerve fibers and the percentage of neurons with fibers longer than 50 μm were calculated from a total of 250-300 neurons per treatment group.

Statistical analysis

All values were expressed as mean ± SEM. When more than three groups were compared, the one-way analysis of variance was chosen to examine differences between groups, and Tukey's multiple comparison test or Student-Newman-Keuls test was selected as a *post-hoc* test where applicable (GraphPad Prism v. 5.01). An unpaired *t*-test with Welch's test is adopted when the two sample groups are unpaired and normally distributed. Moreover, the IC50 of compounds was compared using Extra-sum-of-squares F-tests. Significance was established at $P<0.05$.

Results

1. Analgesic effects of a novel 5-HT_7 antagonist compared to reference standards in IBS-like mouse models

Two models of IBS-like visceral hypersensitivity were used, including the GW model where mice were subjected to a dual trigger of *Giardia* postinfection combined with water avoidance stress, and the PT model of mice post-resolution of trinitrobenzene sulfonic acid-induced colitis (Feng *et al.*, 2012; Lapointe *et al.*, 2015; Hsu *et al.*, 2016; Chang *et al.*, 2022). Intestinal nociception was evaluated in the two mouse models and their respective control groups by measuring VMR values upon colorectal distension (Figures 1A and 1B). We compared the analgesic effects of orally administered CYY, which is a novel and selective 5-HT_7 antagonist, against reference standards used for the treatment of diarrhea-predominant IBS, including ALN (a selective 5-HT_3 antagonist) and LPM (an opioid receptor agonist). Administration of CYY at 5 mg/kg p.o. showed a more potent analgesic effect than ALN and LPM in the two mouse models (Figures 1C and 1D).

Intestinal histology was assessed in the mouse models administered vehicle, CYY, ALN, or LPM. Normal colonic morphology was observed in the GW and PT mouse models and their respective control groups, supporting that intestinal hypernociception was not accompanied by any structural abnormality (Figures 1E and 1F). Moreover, all mice administered CYY or LPM also showed normal intestinal histopathology (Fig. 1E and 1F). Of note, colonic hyperemia and granulocyte infiltration were observed in 28% of the GW mice administered ALN (Fig. 1E). A charcoal meal assay was performed to assess the intestinal transit time in the GW and PT mouse models. No difference in intestinal transit time was observed in mice treated with CYY

or ALN. A decrease in bowel movement was noted after LPM administration in PT mice (Figures 1G and 1H).

2. Distinct patterns of 5-HT receptor subtypes in mouse intestinal mucosa

Immunofluorescent staining was performed to locate the expression of 5-HT receptor subtypes, including 5-HT_3, 5-HT_4, and 5-HT_7, in the colonic tissues of GW and PT mouse models (Figures 2 and 3). Fiber-like staining of PGP9.5 (a pan-neuronal marker) and punctate patterns of 5-HT_7 were noted in the mucosal regions of colonic tissues of GW mice but not of control mice (Figures 2A and 2B). The expression of 5-HT_3 and 5-HT_4 receptors was observed mainly on the epithelia and other cellular structures in the lamina propria of GW mice (Figures 2C and 2D). Quantitative results of fluorescent intensity per area showed elevated PGP9.5 staining in the colonic mucosa of GW mice compared with that of control mice (Figure 2E). Increased mucosal 5-HT_3, 5-HT_4, and 5-HT_7 staining were also observed in colonic tissues of GW mice (Fig. 2E). Moreover, the expression of growth-associated protein 43 (*Gap43*), a marker of neural growth cone, was higher in colonic mucosal samples of GW mice compared with those of control mice by semi-quantitative PCR (Fig. 2F).

For the second model, fiber-like PGP9.5 staining and punctate patterns of 5-HT_7 were found in the colonic mucosa of PT mice (Figures 3A and 3B). The staining of 5-HT_3 was mainly on epithelial and other cells in the lamina propria of Sham and PT mice (Fig. 3C), and low levels of immunoreactivity were noted for 5-HT_4 in the colonic mucosa of Sham and PT mice (Fig. 3D). Quantitative results showed higher levels of mucosal PGP9.5 staining in PT than in Sham mice (Fig. 3E). Moreover, mucosal 5-HT_7 and 5-HT_3 levels were increased in PT mice; comparable 5-HT_4 levels in the colonic mucosa were noted between PT and sham mice (Fig. 3E). Furthermore, a trend of increased *Gap43* expression was also observed in PT mice (Figure 3F).

3. Elevated neurotrophins and neurotrophin receptors associated with mucosal neurite outgrowth in mouse colon tissues

As mucosal neurite outgrowth was evident by PGP9.5 immunostaining in the GW and PT mouse models, we further assessed whether 5-HT_7 expression was localized to enteric nerves by double staining. Colocalization of 5-HT_7 expression with PGP9.5-positive nerve fibers was observed in the mucosal region (Figure 4A). As elevated neurotrophin levels were documented in the biopsy specimens of IBS patients, we next evaluated the levels of neurotrophins and NTRs using qPCR and Western blots in mouse colonic tissues. Higher *Ntrk2* and *Ngfr* gene expression were associated with an increased trend of *Ngf* and *Bdnf* transcripts in GW mice compared with controls (Figure 4B). Elevated *Bdnf* gene expression and an increased trend of *Ntrk2* transcripts

were noted in PT mice (Fig. 4C). A reduction in *Ngfr* gene expression was observed in PT mice (Fig. 4C). Western blotting showed constitutive expression of NGF and BDNF proteins in control mice, suggesting baseline neurotrophin levels in mouse gut tissues (Figures 4D and 4E). However, the protein amounts of NGF and BDNF were only slightly higher in GW and PT mice compared with their respective controls, without statistical significance (Figures 4D and 4E).

4. Stimulation with bacteria-free mouse colonic supernatant and exogenous serotonin increased nerve fiber length in a 5-HT$_7$-dependent manner

A well-established human neuroblastoma cell line, SH-SY5Y, differentiated by retinoic acid was utilized to assess the role of 5-HT$_7$ in nerve fiber extension. The SH-SY5Y cells incubated with bacteria-free colonic supernatant obtained from GW and PT mice showed longer nerve fiber length than those incubated with colonic supernatant from the respective control groups (Figures 5A and 5B). Shorter neurites were observed in those pretreated with CYY *in vitro* at various concentrations (Figures 5A and 5B). In addition, neurons stimulated with exogenous 5-HT and LP-211 (a 5-HT$_7$ agonist) also exhibited longer nerve fibers (Fig. 5C). The average fiber length in each treatment group was quantified from a total of 250-300 neurons and the representative images were shown (Fig. 5D).

Pretreatment with CYY prevented the elongation of nerve fibers induced by mouse colonic supernatant obtained from GW mice in a dose-dependent manner (Figures 6A and 6B). A dose-dependent inhibition of neurite outgrowth by CYY was also found on cells incubated with PT mouse colonic supernatant (Figures 6E and 6F). Another selective 5-HT$_7$ antagonist, SB-269970 (SB7), known to be unstable via oral routes, was tested in the neural cultures *in vitro.* Reduction of neurite length by SB7 was observed in neurons incubated with colonic supernatant from GW (Figures 6C and 6D) and PT mice (Figures 6G and 6H). The IC50 of compounds to suppress neurite outgrowth was calculated, showing that the IC50 doses of CYY were statistically lower than SB7 to suppress nerve fiber elongation caused by incubation with GW supernatant (Figure 6I). However, no differences in IC50 doses were seen between CYY and SB7 when using PT supernatant for incubation with neuron cultures (Fig. 6I). The collective data indicated that gut-derived factors from GW and PT mice were able to promote neurite outgrowth via 5-HT$_7$-dependent pathways.

5. Differential regulatory roles of 5-HT$_3$, 5-HT$_4$, and 5-HT$_7$ in the expression of neurotrophin receptor subunits

We hypothesized that 5-HT stimulation may alter the expression of NTR subunits (TrkA, TrkB, and p75^{NTR}) and examined which serotonin receptor subtypes were

involved in the upregulation of NTRs in neuronal cells. Stimulation with 5-HT elevated *NTRK1, NTRK2,* and *NGFR* gene expression in SH-SY5Y cells (Figures 7A, 7B, and 7C). The 5-HT-induced *NTRK1* upregulation was decreased by CYY and SB7 (selective 5-HT_7 antagonists) but not by ALN (a selective 5-HT_3 antagonist), GR125487 (GR, a selective $5HT_4$ antagonist), or LPM (an opioid receptor agonist) (Figure 7A). The 5-HT-induced *NTRK2* upregulation was partially inhibited by CYY, SB7, ALN, GR, and LPM (Fig. 7B). Moreover, the 5-HT-increased $p75^{NTR}$ expression was reduced by CYY and SB7, whereas ALN or GR had no effect (Fig. 7C). The 5-HT-induced $p75^{NTR}$ upregulation was further increased by pretreatment with LPM (Fig. 7C), suggesting that opioid receptors were involved in the augmentation of serotonin effects on $p75^{NTR}$ expression.

Lastly, SH-SY5Y cells were co-treated with 5-HT and neurotrophins to assess the presence of additive effects on neurite outgrowth on SH-SY5Y cells. Cells treated with a single stimulant of 5-HT or NGF exhibited longer nerve fiber lengths (Fig. 7D). The percentage of neurons with fibers longer than 50 μm was higher after co-treatment with 5-HT and NGF compared with the values of single stimulants (Fig. 7E). Moreover, a single stimulant of 5-HT or BDNF induced neurite outgrowth which was comparable to the fiber length after co-treatment with 5-HT and BDNF (Figures 7F and 7G). Overall, our data indicated that serotonin/5-HT_7 activation upregulated the expression of all three NTR subunits (i.e., TrkA, TrkB, and $p75^{NTR}$), while 5-HT_3 and 5-HT_4 were involved only in TrkB expression. The 5-HT_7 receptor-dependent upregulation of NTR subunits may be involved in mucosal neurite outgrowth and intestinal hyperalgesia (Fig. 7H).

Discussion

IBS represents a substantial clinical problem that accounts for 10-40% of gastroenterology outpatients; however, treatment options for pain management remain limited. Due to the heterogeneous risk factors for IBS development, two experimental models are recommended for nociceptive testing of novel compounds (De Ponti, 2013). Postinfectious and postinflammatory mouse models that showed visceral hypersensitivity upon colorectal distension were assessed in the present study. More potent analgesic effects were observed in the two IBS-like mouse models orally administered a novel 5-HT_7 antagonist, CYY, compared with those given ALN or LPM, reference standards for the clinical management of diarrhea-predominant IBS. We demonstrated that overexpression of 5-HT_7 in mucosal nerve fibers was involved in the pathogenesis of intestinal hypernociception. A new mode of action through upregulation of NTR subunits by 5-HT_7 activation may be involved in neurite outgrowth and intestinal hyperalgesia.

Consistent with the findings of a dense distribution of mucosal nerve fibers in colonic biopsies of IBS patients (Yu *et al.*, 2012; Dothel *et al.*, 2015; Chang *et al.*, 2022),

increased levels of PGP9.5 immunostaining, and neural growth cone marker Gap43 were identified in the intestinal mucosa of two IBS-like mouse models. Intestinal neurite outgrowth was also reported in adult rats after neonatal maternal separation, and in hippocampal neurons of preterm pigs with necrotizing enterocolitis (Barreau *et al.*, 2007; Sun *et al.*, 2018), suggesting the presence of aberrant neuroplasticity in various disorders related to gut-brain axis deficits. Ultrastructural changes of the enteric nervous systems were documented in inflammatory bowel diseases and diverticular diseases (Cervi *et al.*, 2017; Alaburda *et al.*, 2020). We showed that serotonin binding to 5-HT_7 promoted the expression of all three NTR subunits (i.e., TrkA, TrkB, and $p75^{NTR}$), which may potentiate nerve fiber elongation induced by NGF and BDNF. Previous studies using primary hippocampal neurons also demonstrated that 5-HT_7 upregulated TrkB expression and phosphorylation (Samarajeewa *et al.*, 2014). A role of 5-HT_7 in spinogenesis and brain neural development during embryonic and early postnatal stages was previously implicated in anxiety and obsessive-compulsive behaviors (Speranza *et al.*, 2017). In contrast to 5-HT_7, serotonin receptor subtypes 3 and 4 were involved only in the expression of TrkB but not TrkA. The increase in neurotrophins and NTRs in colonic tissues of GW and PT mice was also consistent with the *in vitro* findings. Higher colonic *Ntrk2* and *Ngfr* expression were observed in GW mice, and increased *Bdnf* expression was found in PT mice. However, a reduction in *Ngfr* expression encoding for the low-affinity $p75^{NTR}$ protein was also noted in PT mice. Since the $p75^{NTR}$ in complex with high-affinity TrkA and TrkB is responsible for promoting neuronal cell survival and providing neuroprotective effects (Geetha *et al.*, 2012), the downregulation of $p75^{NTR}$ in PT mice is considered a negative feedback mechanism to curb neurite outgrowth for maintaining homeostasis. In sum, the finding implicated a broader effect of 5-HT_7, amongst the family members of serotonin receptors, on the upregulation of a wide range of NTRs for neuroplasticity.

The expression of 5-HT_3, 5-HT_4, and 5-HT_7 was documented in neuron cells *in vitro* (Schill *et al.*, 2020), but recent evidence showed that 5-HT_{2A}, 5-HT_3, and 5-HT_4 immunoreactivity were also found on the colonic epithelia in humans and mice (Ataee *et al.*, 2010; Spohn *et al.*, 2016; Bhattarai *et al.*, 2017; Bhattarai *et al.*, 2018). Herein, immunofluorescent staining showed increased 5-HT_3 and 5-HT_7 receptor protein levels in the colonic mucosa of GW and PT mice compared with their respective control groups, however, with distinct expression patterns. 5-HT_7 staining was observed on mucosal nerve fibers, in contrast to the mainly epithelial localization of 5-HT_3 and 5-HT_4 in our mouse models. The neuron-specific staining of 5-HT_7 in mouse intestines was consistent with the findings in IBS colonic biopsies (Chang *et al.*, 2022). An increase in mucosal 5-HT_4 expression was observed in GW but not PT mice compared with their control groups, suggesting inconsistent mucosal 5-HT_4 levels depending on the triggers

to induce visceral hypersensitivity. Locally applying a 5-HT_4 agonist increased neuronal cell numbers in the enteric nervous system associated with more stem-like cells in guinea pig ileum (Matsuyoshi *et al.*, 2010) and increased the maturation of dendritic spines in hippocampal neurons (Schill *et al.*, 2020), supporting its role in neuroplasticity. Nevertheless, accumulating evidence from using organoid cultures and animal models indicated that epithelial 5-HT_3 and 5-HT_4 were involved in serotonin-mediated fluid secretion and crypt proliferation (Gross *et al.*, 2012; Bhattarai *et al.*, 2017; Bhattarai *et al.*, 2018; Park *et al.*, 2019). These findings suggested different modes of action and neuron-specific cell types targeted by 5-HT_7 antagonists compared with those exerted by the 5-HT_3 and 5-HT_4 inhibitors.

As IBS is a disorder with high heterogeneity, these findings bring attention to the need for patient subtype stratification for medical prescription. It is noteworthy that a common anti-diarrheal agent, LPM, had opposite effects on the NTR subunits. The activation of opioid receptors on neurons led to decreased TrkB but increased $p75^{NTR}$ expression. LPM works by inhibiting peristaltic activity through direct effects on smooth muscles of the intestinal wall. Early work showed that LPM inhibited the electrically induced contractions of longitudinal muscle strips isolated from guinea pig ileum through direct binding on the mu-opioid receptors on the muscles (Mackerer *et al.*, 1976). Later studies indicated that LPM can inhibit the activity of calcium channels such as high-voltage Ca^{2+} channels and large-conductance Ca^{2+}-activated K^+ channels, and diminish the release of acetylcholine triggered by electrical field stimulation (Burleigh, 1988; Vouga *et al.*, 2021). Overall, LPM inhibition on smooth muscle contraction and acetylcholine release contributes to the general anti-diarrheal effects. The *in vitro* data presented herein indicate that aside from its anti-diarrheal indication, LPM may switch neurotrophin sensitivity from BDNF to NGF by upregulating distinct NTR subunit expression. The finding raised caution for the long-term use of LPM in IBS patients with high neurotrophin levels and dense nerve fibers in the intestinal mucosa.

Mouse models of full *Htr7* gene knockout have been established and they did not show aberrant neuronal development in adulthood (Kim *et al.*, 2013). This suggested that despite its neuromodulatory role, serotonin/5-HT_7 was not accountable for essential functions of neuron survival and differentiation as neurotrophins. In contrast, knockout of the *Ngf* or *Bdnf* gene on both alleles caused prenatal death due to the necessity of NGF and BDNF in neural cell survival (Yu *et al.*, 2012; Dothel *et al.*, 2015; Zhang *et al.*, 2019). Heterozygous BDNF(+/-) or NGF(+/-) mice demonstrated decreased VMR values compared with wild-type controls (Yu *et al.*, 2012; Dothel *et al.*, 2015; Zhang *et al.*, 2019). Moreover, TrkA or TrkB knockout mice exhibited the absence of somatosensory afferents and reduced numbers of neurons in the trigeminal ganglion in oral-facial tissues (Matsuo *et al.*, 2001; Ichikawa *et al.*, 2004). Considering

the necessity of neurotrophin signaling for neuronal survival, therapeutic intervention with a 5-HT_7 antagonist to alleviate pain symptoms could be more beneficial than targeting neurotrophins for IBS management.

In summary, peroral CYY exhibited stronger analgesic effects compared with reference standards in the two IBS-like mouse models. The 5-HT_7-dependent NTR upregulation and neurite outgrowth may be involved in intestinal hypernociception. An orally active novel 5-HT_7 antagonist could be helpful in the management of IBS-like pain.

Figure legends

Figure 1. Comparison of analgesic effects by peroral administration of CYY and reference standards in mice. Two mouse models with IBS-like visceral hypersensitivity were investigated. **(A)** Mice were inoculated with *Giardia* trophozoites on day 0 and subjected to water avoidance stress during the post-clearance phase on days 42-51 (designated the GW model). The control (Ctrl) group were uninfected unstressed animals. In previous studies, giardia colonization during the first week and the self-limiting status of parasite infection were confirmed by the absence of trophozoites around 14-21 days. Mice were subjected to water avoidance stress for ten consecutive days during the post-clearance phase to measure visceromotor responses (VMRs) to colorectal distension by electrode planting into abdominal muscles. **(B)** Mice were intracolonically injected with trinitrobenzene sulfonic acid (TNBS) on day 0, and those that had recovered from TNBS-induced colitis were assessed for VMRs post-TNBS on day 24 (designated the PT model). The sham-injected (Sham) groups were given the same volume of saline on day 0. Persistent pain in the absence of inflammatory parameters or pathological morphology was previously determined in the colonic tissues of the PT model. **(C)** GW mice were orally administered vehicle or reagents such as CYY (a novel 5-HT_7 antagonist), alosetron (ALN, a 5-HT_3R antagonist), or loperamide (LPM, an opioid receptor agonist) at 5 mg/kg before measurement of VMRs to colorectal distension. N=8/group. *$P < 0.05$ *vs.* Ctrl. $^{\#}P < 0.05$ *vs.* vehicle. **(D)** PT mice were orally administered vehicle, CYY, ALN, or LPM before measuring VMRs to colorectal distension. N=8/group. *$P < 0.05$ *vs.* Sham. $^{\#}P < 0.05$ *vs.* vehicle. **(E)** Representative images of the colonic histology of each treatment group in GW mice. Hyperemia (*) and granulocyte infiltration (arrowheads) were observed in the ALN but not in the other groups. N=8/group. **(F)** Representative images of the colonic histology of each treatment group in PT mice. N=8/group. **(G and H)** Treatment with CYY and ALN had no effect on bowel movement whereas LPM decreased intestinal transit time in PT mice. N=8/group. *$P < 0.05$ *vs.* Sham.

Figure 2. Fiber-like patterns of PGP9.5 and 5-HT$_7$ and epithelial staining of 5-HT$_3$ and 5-HT$_4$ were observed in the colonic mucosa of GW mice. Representative immunostaining of **(A)** PGP9.5, **(B)** 5-HT$_7$, **(C)** 5-HT$_3$, and **(D)** 5-HT$_4$ in colonic tissues of Ctrl and GW mice. Puncta- or fiber-like patterns were observed for PGP9.5 and 5-HT$_7$ in mucosal lamina propria, whereas diffuse staining in epithelial layers was noted for 5-HT$_3$ and 5-HT$_4$. Cell nuclei were counterstained with a Hoechst dye (blue) to display tissue orientation. Bar: 50 µm. **(E)** Immunofluorescent intensity per area (µm^2) in gut mucosa. A total of 25 images were used for comparison in each group. * $P < 0.05$, ** $P < 0.01$, *** $P < 0.001$ *vs.* Ctrl. N=5/group. **(F)** Levels of growth-associated protein 43 (Gap43, a marker of neural growth cone) in colon tissues of Ctrl and GW mice as determined by semi-quantitative PCR analysis. * $P < 0.05$ *vs.* Ctrl. N=5/group.

Figure 3. Fiber-like patterns of PGP9.5 and 5-HT$_7$ and epithelial staining of 5-HT$_3$ and 5-HT$_4$ were observed in the colonic mucosa of PT mice. Representative immunostaining of **(A)** PGP9.5, **(B)** 5-HT$_7$, **(C)** 5-HT$_3$, and **(D)** 5-HT$_4$ in colonic tissues of Sham and PT mice. Puncta- or fiber-like patterns were observed for PGP9.5 and 5-HT$_7$ in mucosal lamina propria, whereas diffuse staining in epithelial layers and cellular structures was noted for 5-HT$_3$ and 5-HT$_4$. Cell nuclei were counterstained with a Hoechst dye (blue) to display tissue orientation. Bar: 50 µm. **(E)** Immunofluorescent intensity per area (µm^2) in gut mucosa. A total of 25 images were used for comparison in each group. ** $P < 0.01$, *** $P < 0.001$ *vs.* Sham. N=5-7/group. **(F)** Levels of growth-associated protein 43 (Gap43, a marker of neural growth cone) in colon tissues of Sham and PT mice as determined by semi-quantitative PCR analysis. N=5-7/group.

Figure 4. Higher neurotrophin and receptor levels correlated with increased mucosal nerve fibers expressing 5-HT$_7$ in mice. (A) Representative images showing double staining of PGP9.5 and 5-HT$_7$ in the colonic mucosa of PT mice. Colocalization of PGP9.5 (red) and 5-HT$_7$ (green) immunostaining is shown in the merged images. Bar: 10 µm. N=5/group. **(B and C)** Expression of *Ngf* and *Bdnf* genes and those encoding neurotrophin receptors such as *Ntrk1, Ntrk2,* and *Ngfr* in colon tissues of GW and PT mice compared to their respective controls by qPCR analysis. N=5-7/group. * $P < 0.05$ *vs.* Ctrl or Sham. **(D and E)** Representative Western blots and quantitative results of NGF and BDNF protein levels in colonic mucosal samples of mice. The neurotrophin levels, including precursor and mature forms of NGF, are shown in panel **(a)** and BDNF in panel **(b)**. N=5/group.

Figure 5. Representative mages of neurons after stimulation with colonic

supernatant or exogenous serotonin. Human neuroblastoma SH-SY5Y cells differentiated by retinoic acid (RA) were incubated with bacteria-free mouse intestinal supernatant in the absence or presence of CYY at various concentrations for assessment of nerve fiber length. **(A)** Representative images of neurons following incubation with colonic supernatants of Ctrl and GW mice. Bar: 50 μm. **(B)** Representative images of neurons following incubation with colonic supernatants of Sham and PT mice. Bar: 50 μm. **(C)** Representative images of neurons incubated with exogenous 5-HT (1 μM) and a 5-HT_7 agonist LP-211 (1 μM). Bar: 50 μm. **(D)** Quantitative results of average nerve fiber length in SH-SY5Y cells without treatment (w/o) or after incubation with 5-HT and LP211. A total of 250-300 neurons were used for quantification of nerve fiber length for each group. **P* < 0.05 *vs.* w/o.

Figure 6. Stimulation with mouse colonic supernatant induced neurite outgrowth, which CYY dose-dependently inhibited. Human SH-SY5Y cells were incubated with bacteria-free mouse intestinal supernatant in the presence of CYY or SB-269970 (SB7, a selective 5-HT_7 antagonist) at various concentrations ranging from 0.01 to 100 μM for assessment of nerve fiber length. Average neurite length and the percentage of neurons with neurite longer than 50 μm were measured. **(A and B)** Neurite length following incubation with colonic supernatants of Ctrl and GW mice in the presence of CYY. **P* < 0.05 *vs.* Ctrl. $^{\#}P$ < 0.05 *vs.* GW+ 0 μM. **(C and D)** Neurite length following incubation with colonic supernatants of Ctrl and GW mice in the presence of SB7. **P* < 0.05 *vs.* Ctrl. $^{\#}P$ < 0.05 *vs.* GW+ 0 μM. **(E and F)** Neurite length after incubation with colonic supernatants of Sham and PT mice in the presence of CYY. **P* < 0.05 *vs.* Sham. $^{\#}P$ < 0.05 *vs.* PT+ 0 μM. **(G and H)** Neurite length after incubation with colonic supernatants of Sham and PT mice in the presence of SB7. **P* < 0.05 *vs.* Sham. $^{\#}P$ < 0.05 *vs.* PT+ 0 μM. **(I)** The IC50 of antagonists to suppress neurite outgrowth stimulated by colonic supernatant or exogenous serotonin. A total of 250-300 neurons were used for quantification of nerve fiber length for each group.

Figure 7. Serotonin binding to 5-HT_7 upregulated the expression of neurotrophin receptor subunits to promote neurite elongation. SH-SY5Y cells were stimulated with 5-HT and changes in expression levels of neurotrophin receptor (NTR) subunits were analyzed by qPCR. **(A, B, and C)** SH-SY5Y cells were either untreated or stimulated with 5-HT (1 μM) in the presence of CYY, SB7, alosetron (ALN, a 5-HT_3 antagonist), GR125487D (GR, a 5-HT_4 antagonist), or loperamide (LPM, an opioid receptor agonist). qPCR results of **(A)** *NTRK1,* **(B)** *NTRK2,* and **(C)** *NGFR* gene expression by 5-HT stimulation. **P* < 0.05 *vs.* untreated (UT); $^{\#}P$ < 0.05 *vs.* vehicle (veh). N=6/group. **(D and E)** SH-SY5Y cells were stimulated with recombinant NGF (100 ng/ml) and/or 5-HT (1

μM). Average neurite length and the percentage of neurons with neurites longer than 50 μm after single or co-treatment of NGF and 5-HT. *$P < 0.05$ *vs.* w/o; $^{\#}P < 0.05$ *vs.* NGF. **(F and G)** SH-SY5Y cells were stimulated with recombinant BDNF (100 ng/ml) and/or 5-HT (1 μM). A total of 250-300 neurons were used for quantification of nerve fiber length for each group. *$P < 0.05$ *vs.* w/o. **(H)** Proposed schema of the serotonin/5-HT_7 pathway for upregulation of neurotrophin receptor subunits, including TrkA, TrkB, and $p75^{NTR}$. The 5-HT_7 pathway played a crucial role in promoting mucosal neurite outgrowth and intestinal hypernociception.

REFERENCES

Alaburda P., Lukosiene J.I., Pauza A.G., Rysevaite-Kyguoliene K., Kupcinskas J., Saladzinskas Z., Tamelis A. and Pauziene N. (2020). Ultrastructural changes of the human enteric nervous system and interstitial cells of cajal in diverticular disease. Histol. Histopathol. 35, 147-157.

Ataee R., Ajdary S., Rezayat M., Shokrgozar M.A., Shahriari S. and Zarrindast M.R. (2010). Study of 5HTt3 and HT4 receptor expression in HT29 cell line and human colon adenocarcinoma tissues. Arch. Iran. Med. 13, 120-125.

Atkinson W., Lockhart S., Whorwell P.J., Keevil B. and Houghton L.A. (2006). Altered 5-hydroxytryptamine signaling in patients with constipation- and diarrhea-predominant irritable bowel syndrome. Gastroenterology 130, 34-43.

Barreau F., Cartier C., Leveque M., Ferrier L., Moriez R., Laroute V., Rosztoczy A., Fioramonti J. and Bueno L. (2007). Pathways involved in gut mucosal barrier dysfunction induced in adult rats by maternal deprivation: Corticotrophin-releasing factor and nerve growth factor interplay. J. Physiol. 580, 347-356.

Bhattarai Y., Schmidt B.A., Linden D.R., Larson E.D., Grover M., Beyder A., Farrugia G. and Kashyap P.C. (2017). Human-derived gut microbiota modulates colonic secretion in mice by regulating 5-HT_3 receptor expression via acetate production. Am. J. Physiol. Gastrointest. Liver Physiol. 313, G80-G87.

Bhattarai Y., Williams B.B., Battaglioli E.J., Whitaker W.R., Till L., Grover M., Linden D.R., Akiba Y., Kandimalla K.K., Zachos N.C., Kaunitz J.D., Sonnenburg J.L., Fischbach M.A., Farrugia G. and Kashyap P.C. (2018). Gut microbiota-produced tryptamine activates an epithelial G-protein-coupled receptor to increase colonic secretion. Cell Host Microbe 23, 775-785 e775.

BouSaba J., Sannaa W. and Camilleri M. (2022). Pain in irritable bowel syndrome: Does anything really help? Neurogastroenterol. Motil. 34, e14305.

Burleigh D.E. (1988). Opioid and non-opioid actions of loperamide on cholinergic nerve function in human isolated colon. Eur. J. Pharmacol. 152, 39-46.

Cenac N., Altier C., Motta J.P., d'Aldebert E., Galeano S., Zamponi G.W. and Vergnolle

N. (2010). Potentiation of TRPV4 signalling by histamine and serotonin: An important mechanism for visceral hypersensitivity. Gut 59, 481-488.

Cervi A.L., Moynes D.M., Chisholm S.P., Nasser Y., Vanner S.J. and Lomax A.E. (2017). A role for interleukin 17A in IBD-related neuroplasticity. Neurogastroenterol. Motil. 29, e13112.

Chang W.Y., Yang Y.T., She M.P., Tu C.H., Lee T.C., Wu M.S., Sun C.H., Hsin L.W. and Yu L.C. (2022). 5-HT_7 receptor-dependent intestinal neurite outgrowth contributes to visceral hypersensitivity in irritable bowel syndrome. Lab. Invest. 102, 1023-1037.

Chen T.L., Chen S., Wu H.W., Lee T.C., Lu Y.Z., Wu L.L., Ni Y.H., Sun C.H., Yu W.H., Buret A.G. and Yu L.C. (2013). Persistent gut barrier damage and commensal bacterial influx following eradication of giardia infection in mice. Gut Pathog. 5, 26.

Corsetti M. and Whorwell P. (2017). New therapeutic options for IBS: the role of the first in class mixed μ-opioid receptor agonist and δ-opioid receptor antagonist (mudelta) eluxadoline. Expert Rev. Gastroenterol. Hepatol. 11, 285-292.

De Ponti F. (2013). Drug development for the irritable bowel syndrome: Current challenges and future perspectives. Front. Pharmacol. 4, 7.

Dickson E.J., Heredia D.J. and Smith T.K. (2010). Critical role of 5-HT1A, 5-HT3, and 5-HT7 receptor subtypes in the initiation, generation, and propagation of the murine colonic migrating motor complex. Am. J. Physiol. Gastrointest. Liver Physiol. 299, G144-157.

Dothel G., Barbaro M.R., Boudin H., Vasina V., Cremon C., Gargano L., Bellacosa L., De Giorgio R., Le Berre-Scoul C., Aubert P., Neunlist M., De Ponti F., Stanghellini V. and Barbara G. (2015). Nerve fiber outgrowth is increased in the intestinal mucosa of patients with irritable bowel syndrome. Gastroenterology 148, 1002-1011 e1004.

Dunlop S.P., Hebden J., Campbell E., Naesdal J., Olbe L., Perkins A.C. and Spiller R.C. (2006). Abnormal intestinal permeability in subgroups of diarrhea-predominant irritable bowel syndromes. Am. J Gastroenterol. 101, 1288-1294.

Feng B., La J.H., Tanaka T., Schwartz E.S., McMurray T.P. and Gebhart G.F. (2012). Altered colorectal afferent function associated with TNBS-induced visceral hypersensitivity in mice. Am. J. Physiol. Gastrointest. Liver Physiol. 303, G817-824.

Ford A.C., Sperber A.D., Corsetti M. and Camilleri M. (2020). Irritable bowel syndrome. Lancet 396, 1675-1688.

Ford A.C., Brandt L.J., Young C., Chey W.D., Foxx-Orenstein A.E. and Moayyedi P. (2009). Efficacy of 5-HT3 antagonists and 5-HT4 agonists in irritable bowel syndrome: Systematic review and meta-analysis. Am. J. Gastroenterol. 104, 1831-1843;

771 quiz 1844.
772 Fukudo S., Okumura T., Inamori M., Okuyama Y., Kanazawa M., Kamiya T., Sato K.,
773 Shiotani A., Naito Y., Fujikawa Y., Hokari R., Masaoka T., Fujimoto K., Kaneko H.,
774 Torii A., Matsueda K., Miwa H., Enomoto N., Shimosegawa T. and Koike K.
775 (2021). Evidence-based clinical practice guidelines for irritable bowel syndrome
776 2020. J. Gastroenterol. 56, 193-217.
777 Gao J., Xiong T., Grabauskas G. and Owyang C. (2022). Mucosal serotonin reuptake
778 transporter expression in irritable bowel syndrome is modulated by gut
779 microbiota via mast cell-prostaglandin E2. Gastroenterology 162, 1962-1974
780 e1966.
781 Geetha T., Zheng C., Unroe B., Sycheva M., Kluess H. and Babu J.R. (2012).
782 Polyubiquitination of the neurotrophin receptor p75 directs neuronal cell
783 survival. Biochem. Biophys. Res. Commun. 421, 286-290.
784 Gross E.R., Gershon M.D., Margolis K.G., Gertsberg Z.V., Li Z. and Cowles R.A. (2012).
785 Neuronal serotonin regulates growth of the intestinal mucosa in mice.
786 Gastroenterology 143, 408-417 e402.
787 Halliez M.C., Motta J.P., Feener T.D., Guerin G., LeGoff L., Francois A., Colasse E.,
788 Favennec L., Gargala G., Lapointe T.K., Altier C. and Buret A.G. (2016). Giardia
789 duodenalis induces paracellular bacterial translocation and causes
790 postinfectious visceral hypersensitivity. Am. J. Physiol. Gastrointest. Liver
791 Physiol. 310, G574-585.
792 Hong S., Zheng G., Wu X., Snider N.T., Owyang C. and Wiley J.W. (2011). Corticosterone
793 mediates reciprocal changes in CB 1 and TRPV1 receptors in primary sensory
794 neurons in the chronically stressed rat. Gastroenterology 140, 627-637 e624.
795 Hsu L.T., Hung K.Y., Wu H.W., Liu W.W., She M.P., Lee T.C., Sun C.H., Yu W.H., Buret A.G.
796 and Yu L.C. (2016). Gut-derived cholecystokinin contributes to visceral
797 hypersensitivity via nerve growth factor-dependent neurite outgrowth. J.
798 Gastroenterol. Hepatol. 31, 1594-1603.
799 Huang C.Y. and Yu L.C. (2020). Distinct patterns of interleukin-12/23 and tumor necrosis
800 factor alpha synthesis by activated macrophages are modulated by glucose and
801 colon cancer metabolites. Chin. J. Physiol. 63, 7-14.
802 Huang C.Y., Huang C.Y., Pai Y.C., Lin B.R., Lee T.C., Liang P.H. and Yu L.C. (2019). Glucose
803 metabolites exert opposing roles in tumor chemoresistance. Front. Oncol. 9,
804 1282.
805 Huang Y.J., Lee T.C., Pai Y.C., Lin B.R., Turner J.R. and Yu L.C. (2021). A novel tumor
806 suppressor role of myosin light chain kinase splice variants through
807 downregulation of the TEAD4/CD44 axis. Carcinogenesis 42, 961-974.
808 Ichikawa H., Matsuo S., Silos-Santiago I., Jacquin M.F. and Sugimoto T. (2004). The

development of myelinated nociceptors is dependent upon trks in the trigeminal ganglion. Acta Histochem. 106, 337-343.

Khan N. and Smith M.T. (2015). Neurotrophins and neuropathic pain: Role in pathobiology. Molecules 20, 10657-10688.

Kim J.J. and Khan W.I. (2014). 5-HT7 receptor signaling: Improved therapeutic strategy in gut disorders. Front. Behav. Neurosci. 8, 396.

Kim J.J., Bridle B.W., Ghia J.E., Wang H., Syed S.N., Manocha M.M., Rengasamy P., Shajib M.S., Wan Y., Hedlund P.B. and Khan W.I. (2013). Targeted inhibition of serotonin type 7 (5-HT7) receptor function modulates immune responses and reduces the severity of intestinal inflammation. J. Immunol. 190, 4795-4804.

Kobe F., Guseva D., Jensen T.P., Wirth A., Renner U., Hess D., Muller M., Medrihan L., Zhang W., Zhang M., Braun K., Westerholz S., Herzog A., Radyushkin K., El-Kordi A., Ehrenreich H., Richter D.W., Rusakov D.A. and Ponimaskin E. (2012). 5-HT7R/G12 signaling regulates neuronal morphology and function in an age-dependent manner. J. Neurosci. 32, 2915-2930.

Kuo W.T., Lee T.C. and Yu L.C. (2016). Eritoran suppresses colon cancer by altering a functional balance in toll-like receptors that bind lipopolysaccharide. Cancer Res. 76, 4684-4695.

Kuo W.T., Lee T.C., Yang H.Y., Chen C.Y., Au Y.C., Lu Y.Z., Wu L.L., Wei S.C., Ni Y.H., Lin B.R., Chen Y., Tsai Y.H., Kung J.T., Sheu F., Lin L.W. and Yu L.C. (2015). LPS receptor subunits have antagonistic roles in epithelial apoptosis and colonic carcinogenesis. Cell Death Differ. 22 1590-1604.

Lambarth A., Zarate-Lopez N. and Fayaz A. (2022). Oral and parenteral anti-neuropathic agents for the management of pain and discomfort in irritable bowel syndrome: A systematic review and meta-analysis. Neurogastroenterol. Motil. 34, e14289.

Lapointe T.K., Basso L., Iftinca M.C., Flynn R., Chapman K., Dietrich G., Vergnolle N. and Altier C. (2015). TRPV1 sensitization mediates postinflammatory visceral pain following acute colitis. Am. J. Physiol. Gastrointest. Liver Physiol. 309, G87-99.

Lee J., Avramets D., Jeon B. and Choo H. (2021). Modulation of serotonin receptors in neurodevelopmental disorders: Focus on 5-HT7 receptor. Molecules 26, 3348.

Liu M., Geddis M.S., Wen Y., Setlik W. and Gershon M.D. (2005). Expression and function of 5-HT4 receptors in the mouse enteric nervous system. Am. J. Physiol. Gastrointest. Liver Physiol. 289, G1148-1163.

Mackerer C.R., Clay G.A. and Dajani E.Z. (1976). Loperamide binding to opiate receptor sites of brain and myenteric plexus. J. Pharmacol. Exp. Ther. 199, 131-140.

Matsumoto K., Lo M.W., Hosoya T., Tashima K., Takayama H., Murayama T. and Horie S. (2012). Experimental colitis alters expression of 5-HT receptors and transient

receptor potential vanilloid 1 leading to visceral hypersensitivity in mice. Lab. Invest. 92, 769-782.

Matsuo S., Ichikawa H., Henderson T.A., Silos-Santiago I., Barbacid M., Arends J.J. and Jacquin M.F. (2001). TrkA modulation of developing somatosensory neurons in oro-facial tissues: Tooth pulp fibers are absent in trkA knockout mice. Neuroscience 105, 747-760.

Matsuyoshi H., Kuniyasu H., Okumura M., Misawa H., Katsui R., Zhang G.X., Obata K. and Takaki M. (2010). A 5-HT_4-receptor activation-induced neural plasticity enhances *in vivo* reconstructs of enteric nerve circuit insult. Neurogastroenterol. Motil. 22, 806-813, e226.

Meuser T., Pietruck C., Gabriel A., Xie G.X., Lim K.J. and Pierce Palmer P. (2002). 5-HT7 receptors are involved in mediating 5-HT-induced activation of rat primary afferent neurons. Life Sci.71, 2279-2289.

Michel K., Zeller F., Langer R., Nekarda H., Kruger D., Dover T.J., Brady C.A., Barnes N.M. and Schemann M. (2005). Serotonin excites neurons in the human submucous plexus via 5-HT3 receptors. Gastroenterology 128, 1317-1326.

Monro R.L., Bornstein J.C. and Bertrand P.P. (2005). Slow excitatory post-synaptic potentials in myenteric AH neurons of the guinea-pig ileum are reduced by the 5-hydroxytryptamine7 receptor antagonist SB269970. Neuroscience 134, 975-986.

Nee J., Zakari M. and Lembo A.J. (2015). Current and emerging drug options in the treatment of diarrhea predominant irritable bowel syndrome. Expert Opin. Pharmacother. 16, 2781-2792.

Pai Y.C., Li Y.H., Turner J.R. and Yu L.C. (2023). Transepithelial barrier dysfunction drives microbiota dysbiosis to initiate epithelial clock-driven inflammation. J. Crohns Colitis 17, 1471-1488.

Pai Y.C., Weng L.T., Wei S.C., Wu L.L., Shih D.Q., Targan S.R., Turner J.R. and Yu L.C. (2021). Gut microbial transcytosis induced by tumor necrosis factor-like 1A-dependent activation of a myosin light chain kinase splice variant contributes to IBD. J. Crohns Colitis 15, 258-272.

Park C.J., Armenia S.J., Zhang L. and Cowles R.A. (2019). The 5-HT4 receptor agonist prucalopride stimulates mucosal growth and enhances carbohydrate absorption in the ileum of the mouse. J. Gastrointest. Surg. 23, 1198-1205.

Ren T.H., Wu J., Yew D., Ziea E., Lao L., Leung W.K., Berman B., Hu P.J. and Sung J.J.Y. (2007). Effects of neonatal maternal seperation on neurochemical and sensory reponse to colonic distension in a rat model of irritable bowel syndrome. Am. J. Physiol. Gastrointestinal. Liver Physiol. 292, G849-G856.

Samarajeewa A., Goldemann L., Vasefi M.S., Ahmed N., Gondora N., Khanderia C.,

Mielke J.G. and Beazely M.A. (2014). 5-HT7 receptor activation promotes an increase in TrkB receptor expression and phosphorylation. Front. Behav. Neurosci. 8, 391.

Schill Y., Bijata M., Kopach O., Cherkas V., Abdel-Galil D., Bohm K., Schwab M.H., Matsuda M., Compan V., Basu S., Bijata K., Wlodarczyk J., Bard L., Cole N., Dityatev A., Zeug A., Rusakov D.A. and Ponimaskin E. (2020). Serotonin 5-HT_4 receptor boosts functional maturation of dendritic spines via RhoA-dependent control of F-actin. Commun. Biol. 3, 76.

Speranza L., Labus J., Volpicelli F., Guseva D., Lacivita E., Leopoldo M., Bellenchi G.C., di Porzio U., Bijata M., Perrone-Capano C. and Ponimaskin E. (2017). Serotonin 5-HT7 receptor increases the density of dendritic spines and facilitates synaptogenesis in forebrain neurons. J. Neurochem. 141, 647-661.

Spohn S.N., Bianco F., Scott R.B., Keenan C.M., Linton A.A., O'Neill C.H., Bonora E., Dicay M., Lavoie B., Wilcox R.L., MacNaughton W.K., De Giorgio R., Sharkey K.A. and Mawe G.M. (2016). Protective actions of epithelial 5-hydroxytryptamine 4 receptors in normal and inflamed colon. Gastroenterology 151, 933-944 e933.

Sun J., Pan X., Christiansen L.I., Yuan X.L., Skovgaard K., Chatterton D.E.W., Kaalund S.S., Gao F., Sangild P.T. and Pankratova S. (2018). Necrotizing enterocolitis is associated with acute brain responses in preterm pigs. J. Neuroinflamm. 15, 180.

Tonini M., Vicini R., Cervio E., De Ponti F., De Giorgio R., Barbara G., Stanghellini V., Dellabianca A. and Sternini C. (2005). 5-HT7 receptors modulate peristalsis and accommodation in the guinea pig ileum. Gastroenterology 129, 1557-1566.

Vouga A.G., Rockman M.E., Yan J., Jacobson M.A. and Rothberg B.S. (2021). State-dependent inhibition of BK channels by the opioid agonist loperamide. J. Gen. Physiol. 153.

Yaakob N.S., Chinkwo K.A., Chetty N., Coupar I.M. and Irving H.R. (2015). Distribution of 5-HT3, 5-HT4, and 5-HT7 receptors along the human colon. J. Neurogastroenterol. Motil. 21, 361-369.

Yu F.Y., Huang S.G., Zhang H.Y., Ye H., Chi H.G., Zou Y., Lv R.X. and Zheng X.B. (2016). Comparison of 5-hydroxytryptophan signaling pathway characteristics in diarrhea-predominant irritable bowel syndrome and ulcerative colitis. World J. Gastroenterol. 22, 3451-3459.

Yu L.C., Wei S.C., Li Y.H., Lin P.Y., Chang X.Y., Weng J.P., Shue Y.W., Lai L.C., Wang J.T., Jeng Y.M. and Ni Y.H. (2022). Invasive pathobionts contribute to colon cancer initiation by counterbalancing epithelial antimicrobial responses. Cell. Mol. Gastroenterol. Hepatol. 13, 57-79.

Yu Y.B., Zuo X.L., Zhao Q.J., Chen F.X., Yang J., Dong Y.Y., Wang P. and Li Y.Q. (2012).

Brain-derived neurotrophic factor contributes to abdominal pain in irritable bowel syndrome. Gut 61, 685-694.

Zhang L.Y., Dong X., Liu Z.L., Mo J.Z., Fang J.Y., Xiao S.D., Li Y. and Chen S.L. (2011). Luminal serotonin time-dependently modulates vagal afferent driven antinociception in response to colorectal distention in rats. Neurogastroenterol. Motil. 23, 62-69, e66.

Zhang Y., Qin G., Liu D.R., Wang Y. and Yao S.K. (2019). Increased expression of brain-derived neurotrophic factor is correlated with visceral hypersensitivity in patients with diarrhea-predominant irritable bowel syndrome. World J. Gastroenterol. 25, 269-281.

Zou B.C., Dong L., Wang Y., Wang S.H. and Cao M.B. (2007). Expression and role of 5-HT7 receptor in brain and intestine in rats with irritable bowel syndrome. Chin. Med. J. 120, 2069-2074.

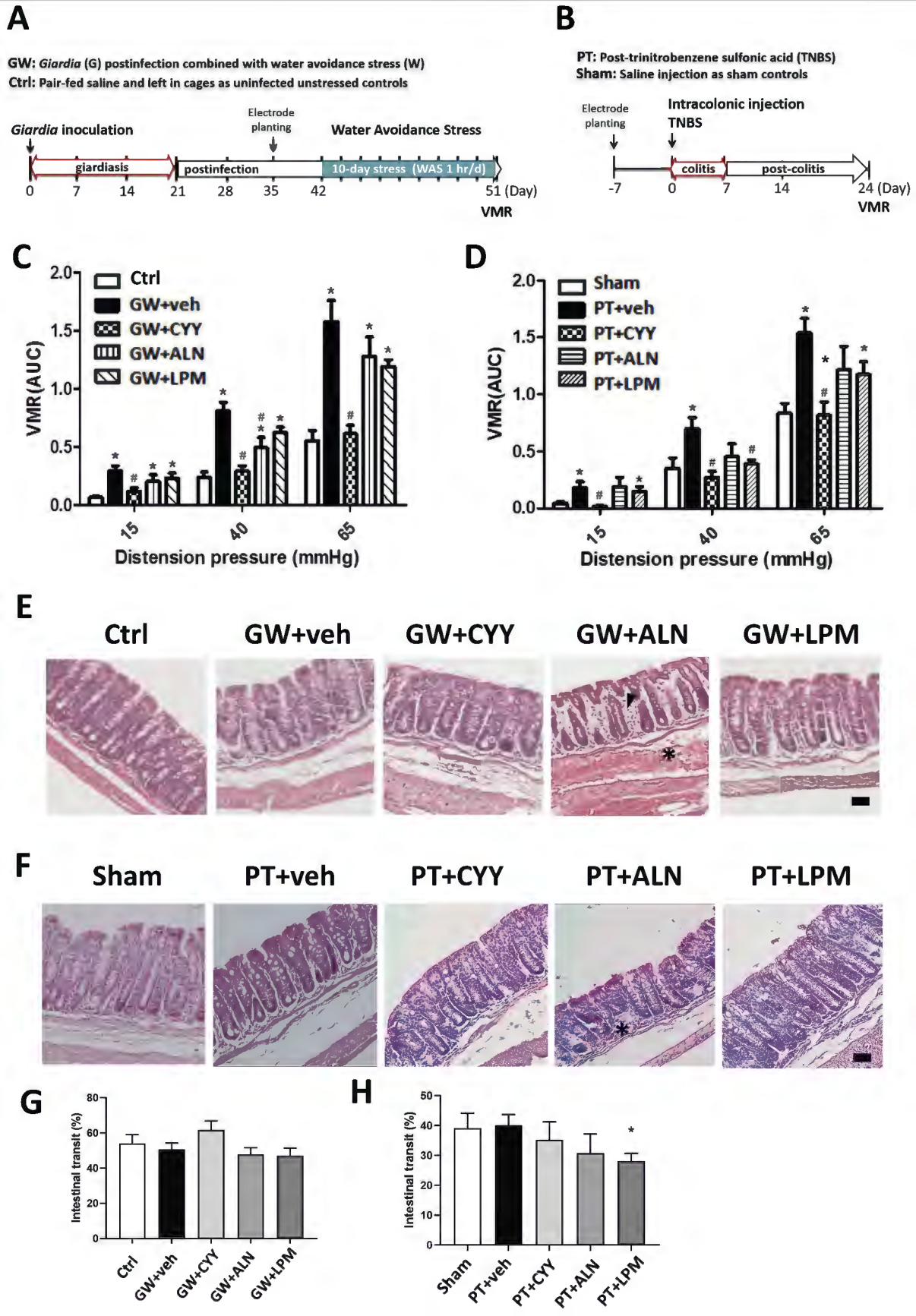
A
GW: Giardia (G) postinfection combined with water avoidance stress (W)
Ctrl: Pair-fed saline and left in cages as uninfected unstressed controls
Giardia inoculation
Electrode planting
Water Avoidance Stress
giardiasis
postinfection
10-day stress (WAS 1 hr/d)
0 7 14 21 28 35 42 51 (Day)
VMR
B
PT: Post-trinitrobenzene sulfonic acid (TNBS)
Sham: Saline injection as sham controls
Electrode planting
Intracolonic injection TNBS
colitis
post-colitis
-7 0 7 14 24 (Day)
VMR
C
Ctrl
GW+veh
GW+CYY
GW+ALN
GW+LPM
VMR(AUC)
Distension pressure (mmHg)
D
Sham
PT+veh
PT+CYY
PT+ALN
PT+LPM
VMR(AUC)
Distension pressure (mmHg)
E
Ctrl
GW+veh
GW+CYY
GW+ALN
GW+LPM
F
Sham
PT+veh
PT+CYY
PT+ALN
PT+LPM
G
Intestinal transit (%)
Ctrl
GW+veh
GW+CYY
GW+ALN
GW+LPM
H
Intestinal transit (%)
Sham
PT+veh
PT+CYY
PT+ALN
PT+LPM

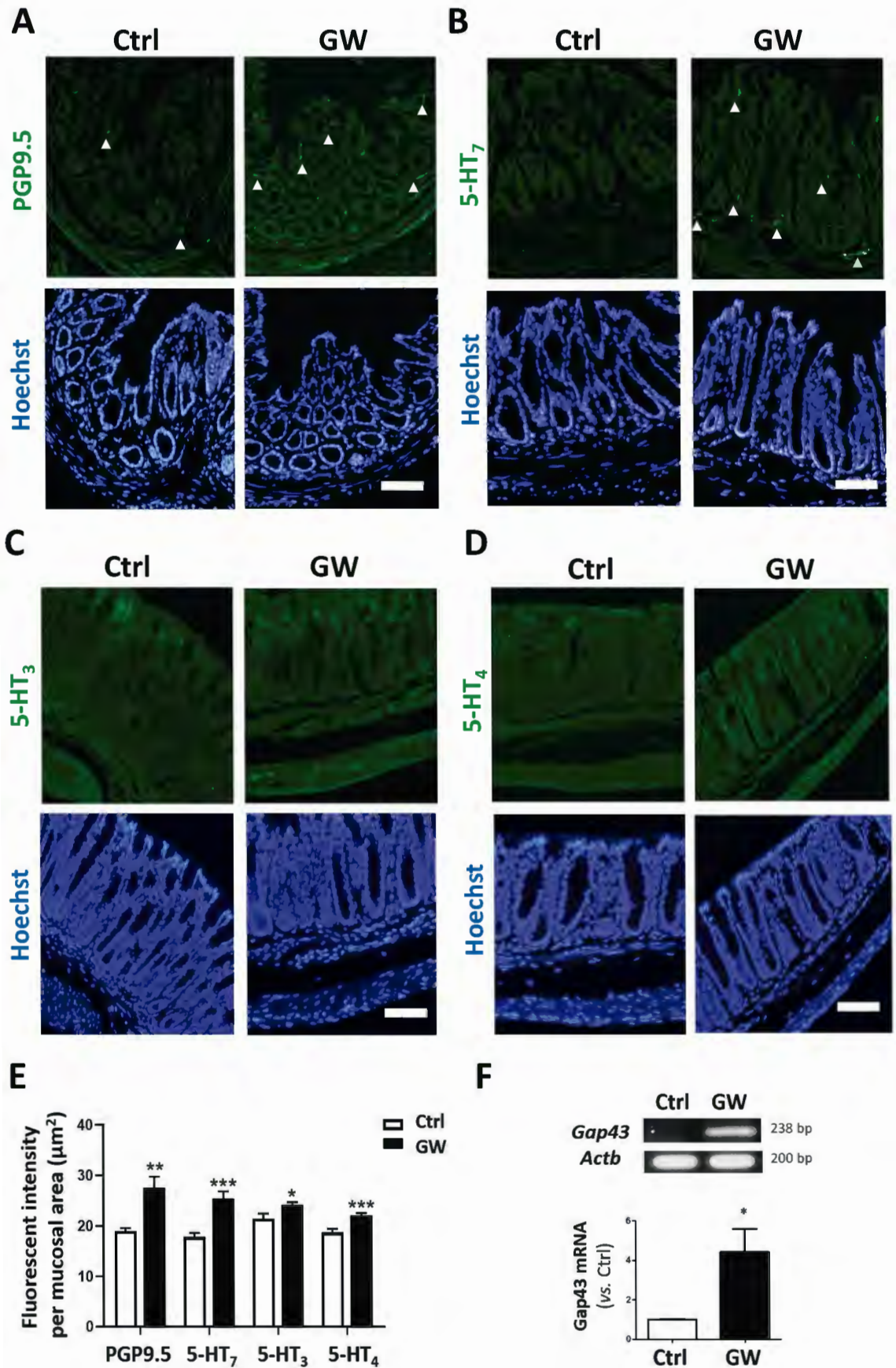
A
Ctrl
GW
PGP9.5
Hoechst
B
Ctrl
GW
5-HT7
Hoechst
C
Ctrl
GW
5-HT3
Hoechst
D
Ctrl
GW
5-HT4
Hoechst
E
Fluorescent intensity per mucosal area (µm²)
40
30
20
10
0
Ctrl
GW
**
***
*
***
PGP9.5
5-HT7
5-HT3
5-HT4
F
Ctrl
GW
Gap43
Actb
238 bp
200 bp
Gap43 mRNA (vs. Ctrl)
6
4
2
0
*
Ctrl
GW

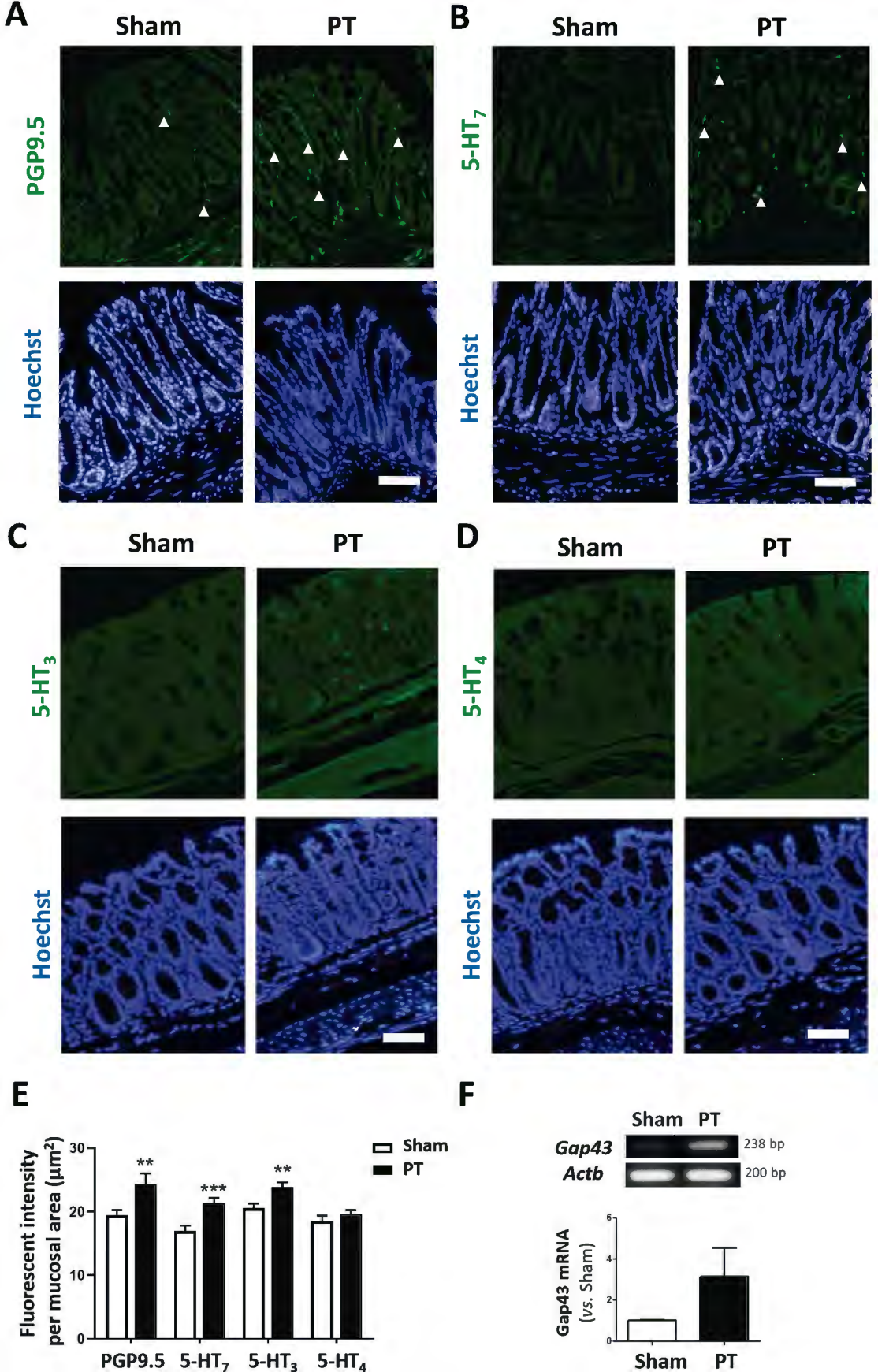
A
Sham
PT
PGP9.5
Hoechst
B
Sham
PT
5-HT7
Hoechst
C
Sham
PT
5-HT3
Hoechst
D
Sham
PT
5-HT4
Hoechst
E
Sham
PT
Fluorescent intensity per mucosal area (µm²)
30
20
10
0
**
***
**
PGP9.5
5-HT7
5-HT3
5-HT4
F
Sham
PT
Gap43
Actb
238 bp
200 bp
Gap43 mRNA (vs. Sham)
6
4
2
0
Sham
PT

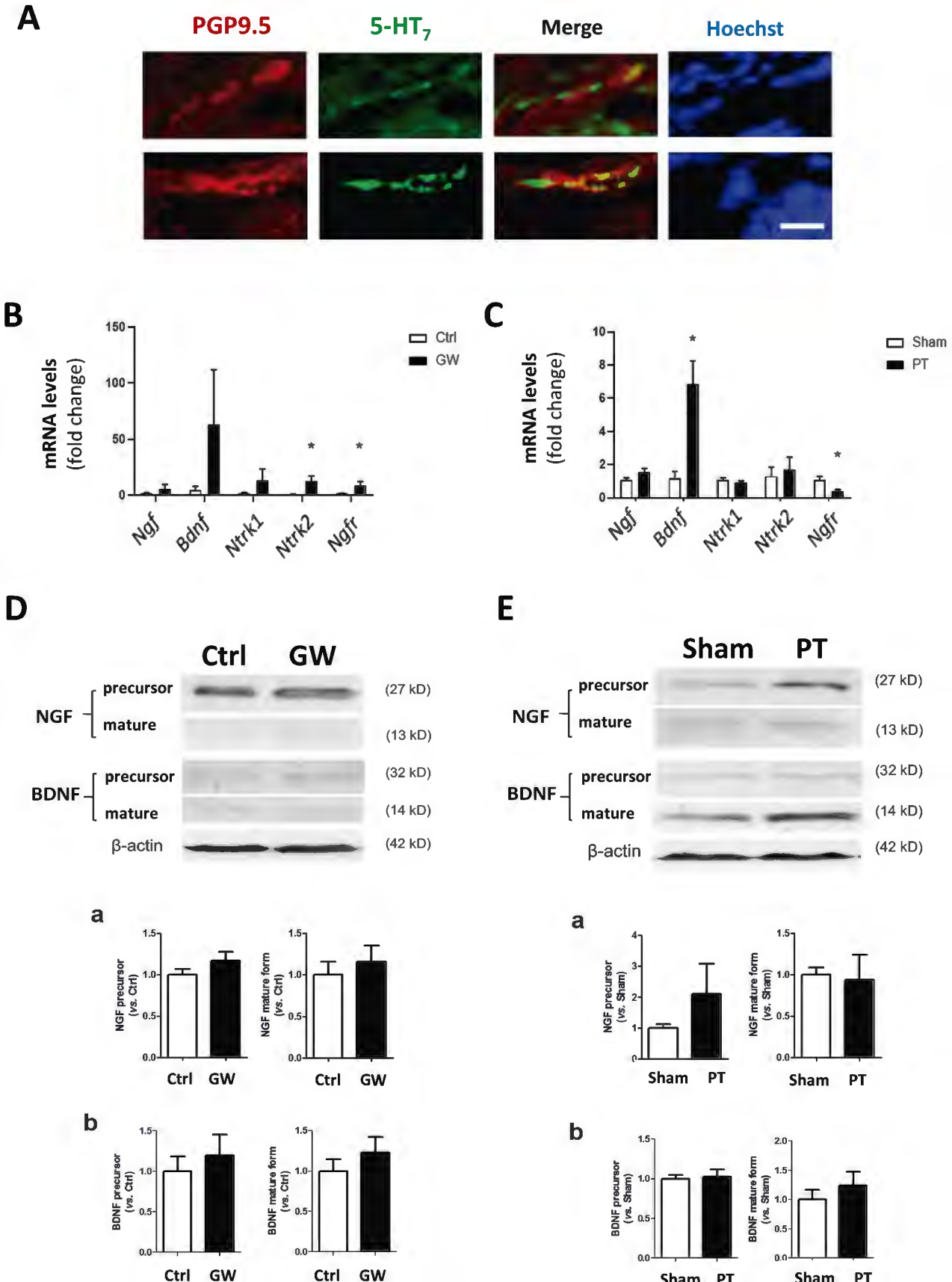
A
PGP9.5
5-HT7
Merge
Hoechst
B
mRNA levels
(fold change)
Ctrl
GW
Ngf
Bdnf
Ntrk1
Ntrk2
Ngfr
C
mRNA levels
(fold change)
Sham
PT
Ngf
Bdnf
Ntrk1
Ntrk2
Ngfr
D
Ctrl
GW
NGF
precursor
mature
(27 kD)
(13 kD)
BDNF
precursor
mature
(32 kD)
(14 kD)
β-actin
(42 kD)
E
Sham
PT
NGF
precursor
mature
(27 kD)
(13 kD)
BDNF
precursor
mature
(32 kD)
(14 kD)
β-actin
(42 kD)
a
NGF precursor (vs. Ctrl)
NGF mature form (vs. Ctrl)
Ctrl
GW
b
BDNF precursor (vs. Ctrl)
BDNF mature form (vs. Ctrl)
Ctrl
GW
a
NGF precursor (vs. Sham)
NGF mature form (vs. Sham)
Sham
PT
b
BDNF precursor (vs. Sham)
BDNF mature form (vs. Sham)
Sham
PT

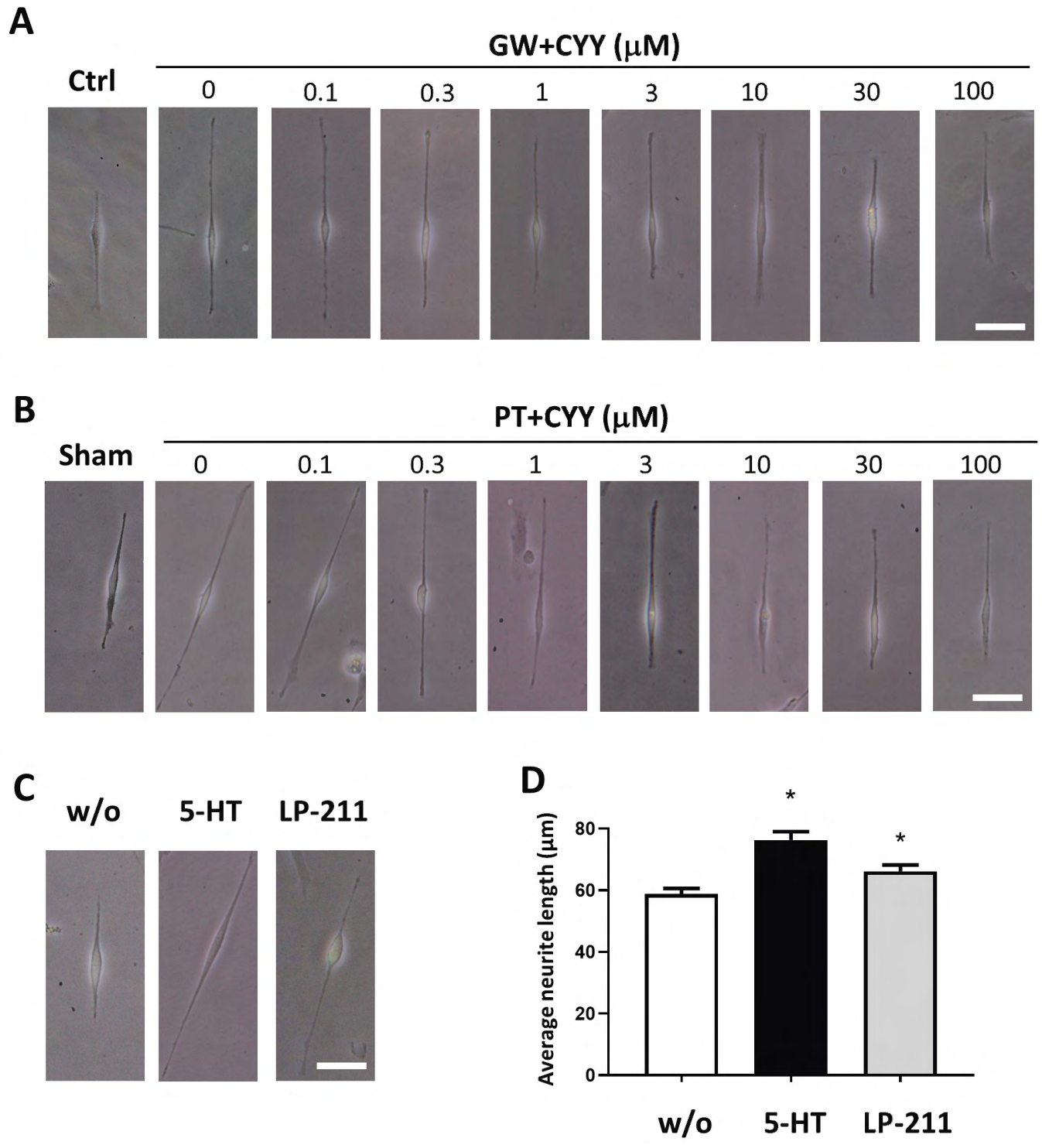
A
GW+CYY (μM)
Ctrl
0
0.1
0.3
1
3
10
30
100
B
PT+CYY (μM)
Sham
0
0.1
0.3
1
3
10
30
100
C
w/o
5-HT
LP-211
D
Average neurite length (μm)
80
60
40
20
0
*
*
w/o
5-HT
LP-211

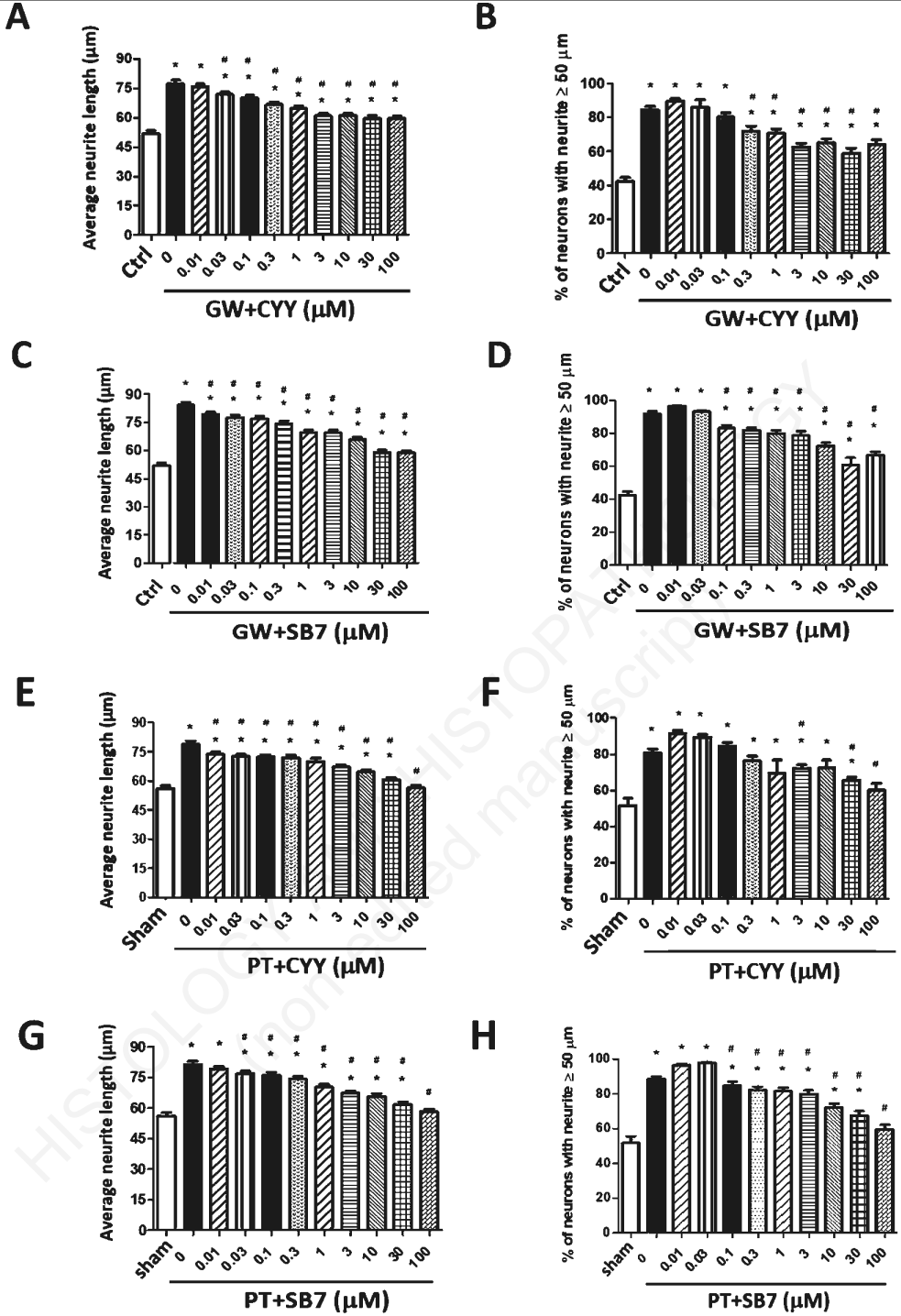

I

IC50	CYY (μM)	SB7 (μM)	*P*-value
Stimulants			
GW colonic supernatant	1.282 ± 0.606	2.919 ± 0.278	0.040
PT colonic supernatant	2.972 ± 0.760	2.130 ± 0.298	0.332

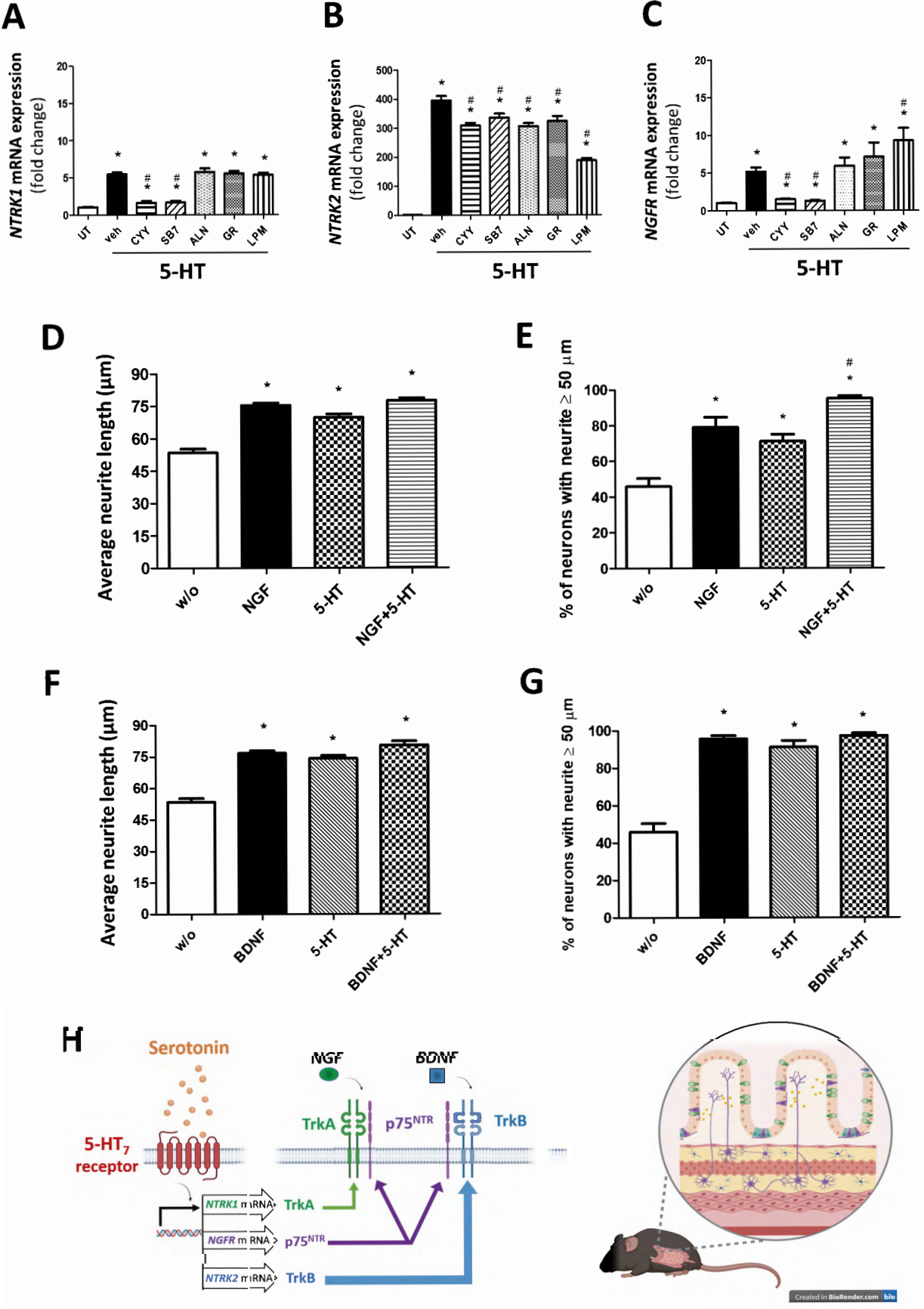
A
NTRK1 mRNA expression (fold change)
UT
veh
CYY
SB7
ALN
GR
LPM
5-HT
B
NTRK2 mRNA expression (fold change)
C
NGFR mRNA expression (fold change)
D
Average neurite length (µm)
w/o
NGF
5-HT
NGF+5-HT
E
% of neurons with neurite ≥ 50 µm
F
BDNF
BDNF+5-HT
G
H
Serotonin
5-HT7 receptor
NGF
BDNF
TrkA
p75NTR
TrkB
NTRK1 mRNA
NGFR mRNA
NTRK2 mRNA
Created in BioRender.com